American Journal of Pathology, Vol. 162, No. 4, April 2003

Disruption of the Caveolin-1 Gene Impairs Renal Calcium Reabsorption and Leads to Hypercalciuria and Urolithiasis

Guangwen Cao,* Guang Yang,* Terry L. Timme,* Takashi Saika,* Luan D. Truong,† Takefumi Satoh,* Alexei Goltsov,* Sang Hee Park,* Taoyan Men,* Nobuyuki Kusaka,* Weihua Tian,* Chengzhen Ren,* Hongyu Wang,* Dov Kadmon,* Wei Wen Cai,‡ A. Craig Chinault,‡ Timothy B. Boone,* Allan Bradley,‡§ and Timothy C. Thompson*¶‖

From the Scott Department of Urology, Department of Pathology,† Department of Human and Molecular Genetics,‡ Department of Molecular and Cellular Biology, Department of Radiology,¶ Baylor College of Medicine,‖ Houston, Texas USA; and the The Sanger Center,§ Wellcome Trust Genome Campus, Cambridgeshire, United Kingdom*

Using *Lox*P/Cre technology, we generated a knockout mouse homozygous for a null mutation in exon 2 of *Cav1*. In male *Cav1*−/− animals, we observed a dramatic increase in the incidence of urinary calcium stone formation. In 5-month-old male mice, the incidence of early urinary calculi was 67% in *Cav1*−/− mice compared to 19% in *Cav1*+/+ animals. Frank stone formation was observed in 13% of *Cav1*−/− males but was not seen in *Cav1*+/+ mice. Urine calcium concentration was significantly higher in *Cav1*−/− male mice compared to *Cav1*+/+ mice. In *Cav1*−/− mice, distal convoluted tubule cells were completely devoid of Cav1 and the localization of plasma membrane calcium ATPase was disrupted. Functional studies confirmed that active calcium absorption was significantly reduced in *Cav1*−/− compared to *Cav1*+/+ male mice. These results demonstrate that disruption of the *Cav1* gene promotes the progressive steps required for urinary calcium stone formation and establish a new mouse model for urinary stone disease. *(Am J Pathol 2003, 162:1241–1248)*

Caveolin-1 (Cav1) is a major structural protein of caveolae, small membrane invaginations of the cell membrane that play a cell and context-dependent role in potocytosis, transcytosis, molecular transport, and signal transduction.[1,2] Specific molecules from four major signaling pathways have been detected in caveolae, G-protein mediated signaling, calcium-mediated signaling, tyrosine kinase/mitogen-activated protein kinase signaling, and lipid signaling. Caveolae appear to be a focal point for compartmentalizing, organizing, and modulating signal transduction activities that begin at the cell surface and Cav1 may function not only as a structural molecule but also to modulate the function of signal transduction pathways.[2] Given the complexity of each signal transduction pathway and the potential for cross talk and interactions between pathways it is likely that Cav1 may be uniquely associated with specific pathological responses in individual cell types. We have documented increased expression of Cav1 in prostate cancer, especially metastatic and androgen-insensitive disease.[3–7] To further investigate the functions of Cav1 we generated mice with deletions of the *Cav1* gene.

In this report we describe generation of *Cav1*−/− mice and the unique observation that male *Cav1*−/− mice develop hypercalciuria and urolithiasis. In humans, some urinary calculi occur as a result of foreign bodies, obstruction, or infection but many are a result of stone formation in the kidney or a reflection idiopathic hypercalciuria.[8] Indeed, treatment options for recurrent stone formation in men with idiopathic hypercalciuria has been the subject of some controversy with a recent study suggesting that prevention with a diet low in protein and salt rather than calcium is most effective.[9] Certain rare X-linked recessive diseases such as Dent's disease are accompanied by nephrolithiasis that has been linked to mutations in a voltage-gated chloride channel. Two mouse models of this disease syndrome were established.[10,11] Both models had proteinuria but only one also had hypercalciuria with microscopic calcium deposits in the kidney[11] and the occurrence of calculi was not reported. Our studies point to Cav1 function as a critical determinant of urinary calcium homeostasis and demonstrate that homozygous deletion of the *Cav1* gene can lead to formation of urinary calculi.

Supported by Public Health Service grants U01-CA84295, P50-CA58204, and RO1-CA68814 from the National Cancer Institute. A portion of these studies were conducted in facilities provided by the Houston VA Medical Center.

Accepted for publication January 8, 2003.

Address reprint requests to Timothy C. Thompson, Ph.D., Scott Department of Urology, Baylor College of Medicine, 6560 Fannin Suite 2100, Houston, TX 77030. E-mail: timothyt@www.urol.bcm.tmc.edu.

Materials and Methods

Generation of Embryonic Stem Cells with Deleted Cav1 Exon 2

A 129/Sv mouse genomic library (Stratagene, La Jolla, CA) was screened with a mouse *Cav1* cDNA probe.[3] Exon/intron boundaries were determined by means of restriction mapping and DNA sequencing. We isolated and characterized a 4.5Kb *Eco*RI genomic clone containing *Cav1* exon 1 and exon 2. To generate the targeting vector, A cassette expressing the neomycin resistance gene (neo^R) flanked by two *Lox* P sites (GenBank accession number AF335420) was placed in upstream of exon 2 (*Nhe*I site) and another *Lox*P site was inserted into intron 2 (*Nde*I site). A thymidine kinase (tk) cassette was inserted downstream in the vector. We electroporated AB2.2 embyonic stem (ES) cells with the *Bam*HI linearized targeting vector and identified targeted ES cell clones by Southern blot analysis using probes external to the targeting vector.[12] Electroporation with a Cre-expression plasmid, pCMV-Cre, mediated recombination between two *Lox*P sites deleting DNA sequences flanking exon 2. We screened clones containing deleted and "floxed" mutant alleles by Southern blot analysis. Protein analysis by Western blotting was as previously described[3] using rabbit anti-Cav1 (Santa Cruz Biotechnology, Santa Cruz, CA), mouse anti-Cav2 (Transduction Labs, San Diego, CA), or mouse anti-Cav3 (Transduction Labs).

Generation and Identification of Cav1 Mutant Mice

Targeted ES cell clones were used to create chimeras. Chimeric males were mated with C57Bl6/J $Tyr^{c\text{-}Brd}$ females and germline transmission of the mutant allele was verified by Southern blot analysis of genomic DNA from pigmented F1 offspring. Mice from *Cav1*+/− intercrosses were genotyped by PCR. Primers (Figure 1A) were intron1 sense, **F1**, 5′-TTCTGTGTGCAAGCCTTTCC-3′, exon 2 antisense, **R1**, 5′-GTGTGCGCGTCATACACTTG-3′ and targeting vector antisense, **R2**, 5′-GGGGAGGAGTAGAAGGTGGC-3′. All mice used in the experiments were F2-F4 hybrids and were maintained in facilities accredited by the American Association for Accreditation of Laboratory Animal Care and all experiments conducted in accordance with the principles and procedures outlined in the National Institutes of Health's Guide for the Care and Use of Laboratory Animals.

Histopathology and Immunohistochemistry

Animals were euthanized and after careful observation for gross changes organs were dissected and weighed. Tissue samples were fixed in 10% buffered formalin and embedded in paraffin. Kidney sections (4 to 5 μm) were stained with hematoxylin and eosin (H&E) according to standard protocols and were evaluated microscopically. Immunohistochemical analysis for Cav1 was as previously described.[3,13] Antibody to plasma membrane calcium ATPase (PMCA) was from Affinity Bioreagents (Golden, CO) and Na^{++}/Ca^{++} exchanger antibody was from Swant (Switzerland). Calbindin D_{28K} antibody was from Sigma-Aldrich (St. Louis, MO). Antibody reactivity was detected by standard ABC immunostaining or immunofluorescence for double labeling with Cav1 and PMCA antibodies. The Von Kossa histochemical stain was used to demonstrate calcification in urinary calculi.[14]

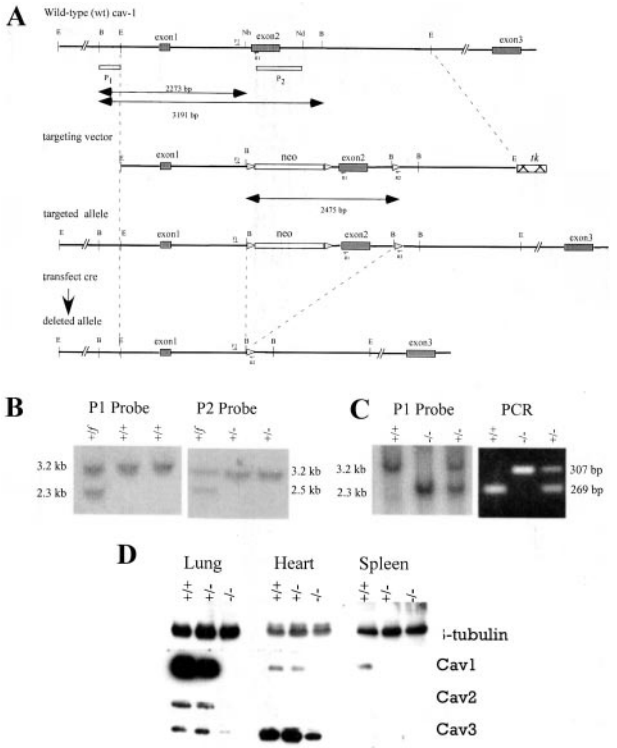

Figure 1. Disruption of mouse *Cav1*. **A:** Structure of targeting vector and partial restriction map of *Cav1* exon 2 locus before and after homologous recombination and Cre-mediated recombination. Exons are indicated by **black boxes**. The location of Southern blot probes (P1, P2) is represented by **empty boxes**. *Lox* P sites are represented by **empty triangles**. Different mutant alleles of exon 2 after gene targeting and Cre-mediated recombination are shown. Three primers (F1, R1 and R2) were used for detection of deleted alleles. **B:** Southern blot analysis of *Cav1 Lox*P3 ES clone, *Lox*P2 and *Lox*P1 ES clones after digestion. The genotype of individual ES clones is indicated on the top of the gel. **C:** Genotype of offspring from *Cav1*+/− intercrosses analyzed by Southern blot and PCR. **D:** Total protein from lung, heart and spleen of (+/+), (+/−), and (−/−) animals was examined by Western blotting with β-tubulin, Cav1, Cav2, or Cav3 antibody.

Biochemical Analyses

Urine was collected over a 24-hour period by means of metabolic cages (Nalgene, Rochester, New York). Blood was collected by major venous puncture at the time of euthanasia. Urine and serum chemical analyses were performed at the Baylor Department of Pathology using Roche Cobas Mira (GMI, Inc, Albertville, MN). Calculi were analyzed by the Baylor Urolithiasis Laboratory.

In Vivo Calcium Reabsorption Test

The effect of a Ca^{++} restriction on the urinary excretion of Ca^{++} was essentially as described.[15] Five-month-old

male mice were fed a Ca^{++}, Mg^{++}-deficient diet (Harlan Teklad, Indianapolis, IN) for 4 days while in metabolic cages and urine collected every 24 hours.

Results

To elucidate the role of Cav1 *in vivo* and minimize a possible influence of any antibiotic selection genes in mutant animals, we specifically deleted one allele of *Cav1* exon 2 together with possible splicing sites, covering the 5′ coding regions of both *Cav1α* and *Cav1β* mRNA[16] in embryonic stem (ES) cells (Figure 1A). ES cells were electroporated with the targeting vector and G418-resistant ES cell clones screened by Southern blot analysis using a probe (P1) external to the targeting vector (Figure 1B). Two targeted ES cell clones were electroporated with a Cre expression vector and isolated clones were screened by Southern blotting with probe P2 (Figure 1A) and several clones were identified which had a deletion of exon 2 and Neo (Figure 1B). One of these ES cell clones contributed to the germ line of chimeric mice which yielded *Cav1*+/− F1 offspring. Heterozygous mice were intercrossed and their offspring genotyped (Figure 1C). From a total of 2296 mice, 587 were *Cav1*+/+ (24.7%), 1189 were *Cav1*+/− (51.8%) and 540 were *Cav1*−/− (23.5%), close to the expected Mendelian ratio (1:2:1), indicating the viability of homozygous mice. The mean body weight of *Cav1* −/− mice ($28.6 \pm 0.6 \times g$) and *Cav1*+/+ mice ($27.5 \pm 0.5 \times g$) was not significantly different at 5 months ($P = 0.1636$, $n = 72$) or at other ages. *Cav1*−/− mice were fertile and had a normal litter size and gender ratio. Western blot analysis of total protein from heart, spleen and lung confirmed the absence of Cav1 protein in *Cav1*−/− mice (Figure 1D). As previously reported[17–19] expression of Cav2 was also affected in Cav1+/− and −/− lung and heart. The expression of Cav3 in the heart of our Cav1−/− mice appeared to be reduced to the same extent as that shown by Zhao et al,[19] but in contrast to the mice reported by Drab et al[17] in which Cav3 expression in the heart appeared unchanged.

Histopathological examination of *Cav1*−/− mice, compared to +/− and +/+ littermates, revealed tissue abnormalities consistent with those previously reported, eg, lung abnormalities.[17–19] Surprisingly, in several *Cav1*−/− male mice that were 4 months old we found urinary bladder calculi. To systematically investigate this observation we performed a thorough examination of *Cav1*−/− and +/+ mice at four specific ages (Figure 2). Two categories of urinary calculi were observed, early urinary calculi with relatively abundant matrix debris as well as frank solid stones. In 5-month-old *Cav1*−/− male mice overall urinary calculi formation within the bladder was observed in 80% of the mice whereas in *Cav1*+/+ male mice of the same age the frequency was only 19%. Within these groups early urinary calculi were observed in 67% of the *Cav1*−/− male mice and 19% of the *Cav1*+/+ male

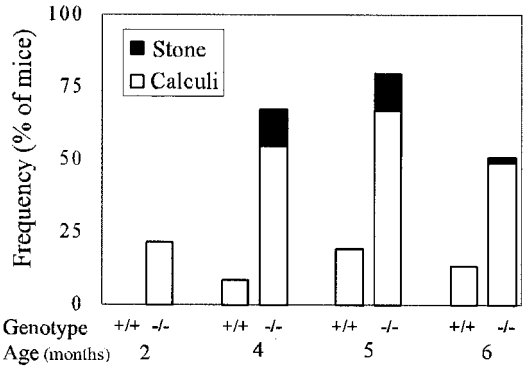

Figure 2. The frequency of early urinary calculi (**open boxes**) and solid stones (**solid boxes**) in male mice in four age groups. The number of mice in each group varied from 23 to 60.

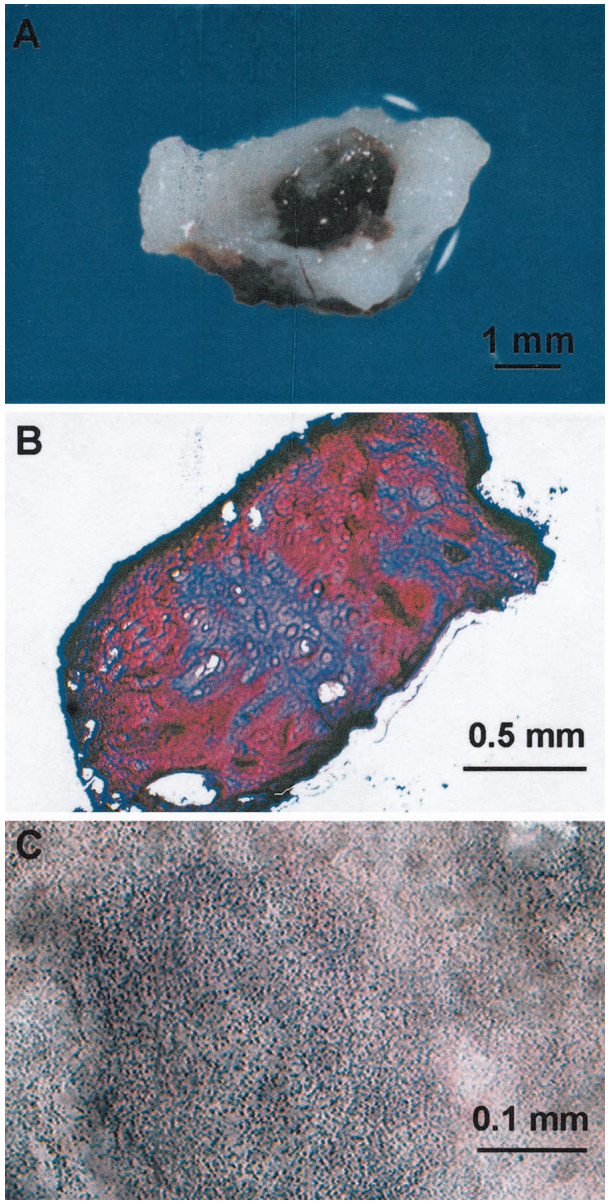

Figure 3. Urinary calculi and stones. **A:** In *Cav1*−/− animals, solid calcium phosphate stones could be identified in urinary calculi. **B:** H&E staining of calculi revealed a pinkish staining for calculi proteins with central light bluish staining representing potential calcification. **C:** Von Kossa staining demonstrated the granular calcium deposits in the calculi. Size of **bars** indicated.

Table 1. Biochemical Analysis of Urine and Serum

	Sex	Cav1 +/+	n	Cav1 −/−	*n*	*P* value*
Urine calcium (mg/dl)	M	7.1 (± 1.0)	16	15.0 (± 2.5)	17	0.008
	F	9.7 (± 1.3)	5	9.2 (± 1.6)	6	0.814
Urine creatinine (mg/dl)	M	92.1 (± 35)	18	77.7 (± 11)	18	0.695
	F	61.2 (± 10)	10	89.8 (± 10)	10	0.068
Urine total protein (g/dl)	M	2.2 (± 0.4)	14	1.8 (± 0.3)	14	0.399
	F	0.98 (± 0.2)	10	0.67 (± 0.2)	10	0.227
Serum calcium (mg/dl)	M	13.0 (± 0.4)	7	13.0 (± 0.4)	8	0.841
Serum creatinine (mg/dl)	M	0.6 (± 0.03)	7	0.7 (± 0.06)	8	0.301
Blood urea nitrogen (mg/dl)	M	26.8 (± 0.8)	5	26.8 (± 1.6)	6	0.980
Serum phosphorus (mg/dl)	M	14.4 (± 1.9)	5	17.9 (± 2.9)	6	0.361
Serum albumin (g/dl)	M	3.6 (± 0.7)	5	3.4 (± 0.2)	6	0.848
Serum total protein (g/dl)	M	6.8 (± 0.3)	5	6.7 (± 0.2)	6	0.868

**P* value determined with Student's t test.

mice and frank urinary stones were seen in 13% of the *Cav1*−/− mice at 5 months of age and none of the +/+ mice at any age analyzed. Urinary calculi or stones were not observed in female *Cav1*−/− ($n = 53$) or *Cav1*+/+ ($n = 49$) mice at any age (data not shown). Urinary calculi were usually heterogeneous in composition (Figure 3A) and chemical analysis of seven solid stone samples indicated that four contained calcium phosphate and/or calcium oxalate and six samples contained nonspecific cellular/organic material. Hematoxylin and eosin staining revealed that the calculi were composed of a non-cellular, pinkish substance with focal hematoxylin-stained precipitation suggesting potential calcification (Figure 3B). To further analyze calculi in which ostensible solid stone formation was not apparent, all calculi from the 5-month age group of male mice were analyzed by Von Kossa staining which is capable of potentially identifying calcium deposition (Figure 3C). Positive Von Kossa staining was demonstrated in 31% of the urinary calculi from *Cav1*−/− male mice, whereas negative Von Kossa staining was observed in all *Cav1*+/+ urinary calculi. Histological examination did not reveal any microscopic dystrophy of the bladder muscle. Overall, the data are consistent with progressive microscopic calcium deposition and ostensible stone formation in male *Cav1*−/− mice but not in *Cav1*+/+ littermates.

To examine if urine composition was playing a role in stone formation, 24-hour urine samples were collected using a metabolic cage for chemical analysis. Urinary Ca^{++} in *Cav1*−/− male mice was significantly higher than that of *Cav1*+/+ littermates whereas (Table 1). Interestingly, urinary Ca^{++} levels in *Cav1*−/− female mice were similar to those in *Cav1*+/+ females. Urinary creatinine or total protein were not significantly different between *Cav1*−/− and *Cav1*+/+ animals whether male or female. Microscopic crystals together with heterogeneous material were observed in the urine of all male *Cav1*−/− mice but not *Cav1*+/+ mice (data not shown). Neither calculi nor calcifications were found in the renal parenchyma, pyelocaliceal system or ureter of any *Cav1*−/− mouse when tissue sections were carefully evaluated after H&E, periodic acid Schiff, or von Kossa staining. Surprisingly no features of cell injury were found in any renal tubular segment. In addition there were no glomerular or vascular changes and no evidence of Randall's plaques.[20] As expected, serum Ca^{++} levels were not significantly different. High urine Ca^{++} and normal serum Ca^{++} were suggestive that *Cav1*−/− male mice might have defects in renal Ca^{++} absorption or excretion.

Analysis of the kidneys revealed that the kidney weight in *Cav1*−/− male mice (220 ± 6 mg) was significantly higher than in age and body weight-matched *Cav1*+/+ males (201 ± 6 mg, $P = 0.0141$), however, there were no significant differences at the microscopic level in cell density, or morphology of the glomeruli and tubule cells (data not shown). Immunohistochemical analysis did not demonstrate detectable IgG precipitate within the glomeruli (data not shown), suggesting that the calcium filtration disorder was not related to autoimmune glomerulonephritis.[21]

Immunohistochemical analysis of *Cav1*+/+ (Figure 4, A-C) and *Cav1*−/− (Figure 4, D-F) male mice indicated that Cav1 expression was predominantly localized to the basal area of the distal convoluted tubule (DCT) cells in *Cav1*+/+ kidney, consistent with localization studies in Sprague-Dawley rats,[22] but was completely absent in *Cav1*−/− kidney. PMCA, an important basolateral $Ca2^{+}$ active transporter in DCT cells,[23] was also evaluated by immunohistochemistry. The data indicated that in *Cav1*+/+ animals PMCA was detected in the cytoplasm and tended to concentrate in the basolateral region of the DCT epithelia (Figure 4B). In contrast, this polarity in cellular distribution was absent in the *Cav1*−/− male (Figure 4E) and female kidneys (not shown). Immunohistochemical analysis of calbindin D_{28k}, a major cytoplasmic calcium-binding protein, demonstrated similar intensity and cytoplasmic distribution in *Cav1*+/+ and

Figure 4. Immunocytochemical assessment of male *Cav1*+/+ (**A**, **B**, and **C**) or *Cav1*−/− kidney tissue (**D**, **E**, and **F**). Cav1 expression was predominantly identified in the basal area of DCT of *Cav1*+/+ kidney (**A**) and completely absent in a *Cav1*−/− kidney (**D**). PMCA immunoreactivity was detected in the cytoplasm of distal tubular epithelia where it tended to concentrate at the basolateral region in *Cav1*+/+ kidney DCT cells (**B**). This polarity in cellular distribution disappeared in *Cav1*−/− DCT cells (**E**). A similar calbindinD_{28k} expression pattern was seen in distal tubules of both *Cav1*+/+ (**C**) and *Cav1*−/− (**F**) kidney. Double immunofluorescence labeling of Cav1 (**G**) and PMCA (**H**) in a *Cav1*+/+ kidney indicated that the two proteins were partially co-localized (**I**). **Bar**, 125 μm in **A, C, D,** and **F**; **bar**, 60 μm in **B, E,** and **G– I**.

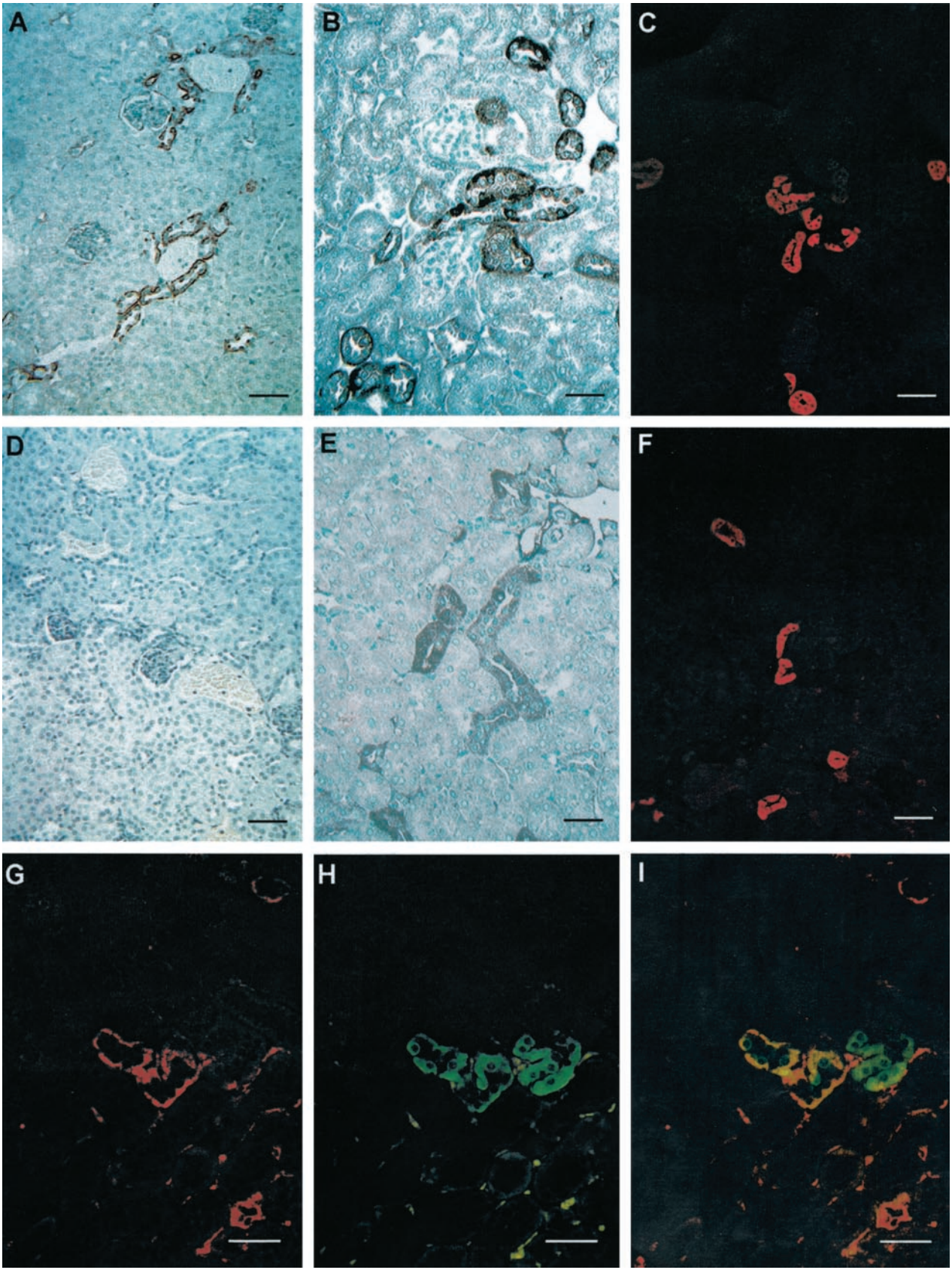
A
B
C
D
E
F
G
H
I

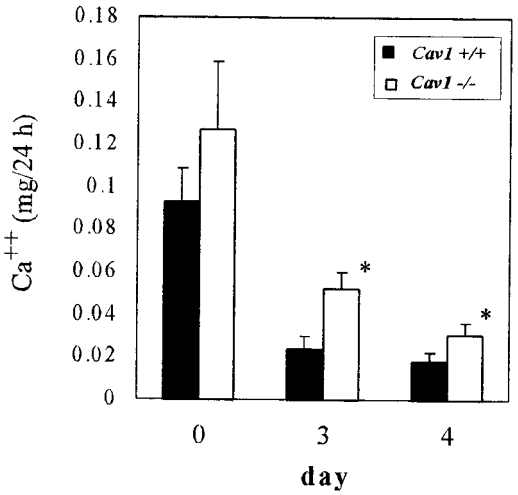

Figure 5. Calcium reabsorption analysis in male mice. Urine Ca^{++} expressed as mg of Ca^{++} per 24 hours before (day 0) and after 3 or 4 days on a Ca^{++}, Mg^{++}-deficient diet. Renal function, as assessed by creatinine remained normal. *, $P = 0.0279$ on day 3 and 0.0454 on day 4.

Cav1−/− kidney (Figure 4, C and F, respectively), as did the Na^+/Ca^{++} exchanger (data not shown). To determine whether Cav1 and PMCA might interact we performed double immunofluorescent staining for Cav1 (Figure 4G) and PMCA (Figure 4H) in *Cav1*+/+ kidney sections. In the superimposed image (Figure 4I) the two proteins co-localize in some areas.

Since our data suggested that Ca^{++} reabsorption from urine and transport into blood might be compromised in *Cav1*−/− animals, we performed a metabolic study of male mice fed a Ca^{++}, Mg^{++}-deficient diet.[15] Twenty-four hour urine calcium output as standardized by creatinine is shown in Figure 5. Basal Ca^{++} levels in *Cav1*−/− male mice were significantly higher than in *Cav1*+/+ controls as detected in previous studies (Table 1). After 3 days on the Ca^{++}, Mg^{++}-deficient diet, total Ca^{++}/creatinine levels in both groups were considerably decreased with the level in *Cav1*+/+ mice barely detectable and the *Cav1*−/− group significantly higher (Figure 5), indicating that Ca^{++} active absorption was impaired. Renal function assessed as creatinine clearance remained essentially normal during this process, and urine protein excretion was not significantly different between the two groups (data not shown).

Discussion

Urolithiasis, which often affects males to a much greater extent than females, is a multifaceted process. Several steps are required for the generation of frank calcium oxalate or calcium phosphate stones. Calcium oxalate crystals are often found in the urine in healthy subjects indicating that crystallogenesis is controlled such that small crystals are usually swept out by the urine without leading to pathological consequences. The events leading to formation of large crystal aggregates are poorly understood. Urinary proteins play an important role in stone formation by serving as a nidus that leads to the subsequent formation of a larger crystalline matrix structure and ultimately ostensible stone formation.[24–26] In addition to the presence of proteins, hypercalciuria is the most common metabolic abnormality in patients with urolithiasis. Increased urine calcium excretion was the only phenotype associated with the kidney stone formation in a family-based study.[27] The frequency of hypercalciuria in men and women with a history of kidney stone disease is much higher than that of normal counterparts.[28] Defects in calcium absorption are an important cause of hypercalciuria in normocalcemic patients[29] and in a genetic hypercalciuric stone-forming rat model.[30] Active calcium absorption involves passive entry through apical membrane calcium channels followed by active transport across basolateral plasma membranes within the distal part of the nephron. The latter is mediated by means of PMCA and a Na^+/Ca^{++} exchanger.[31] Immunohistochemical studies have localized the basolateral Ca^{++} transporting proteins, and the cytoplasmic Ca^{++} binding protein calbindinD_{28K} and an apical epithelial Ca^{++} channel are enriched exclusively in DCT.[13]

In our study, we found an increased percentage of urinary calculi in the bladders of male *Cav1*−/− mice beginning at 2 months of age and the incidence of urinary calculi increased with age. Although bladder stone formation occurs in humans, the presence of stones within renal calices is far more common in the Western hemisphere.[32] The reasons for the exclusive presentation of bladder but not renal calculi in *Cav1*−/− male mice is unclear at this time. Female *Cav1*−/− mice did not experience urolithiasis. Interestingly, male but not female mice of the same strain (129/Sv) have been reported to develop early calculi in an age-dependent manner[33] confirming that this strain of mice is somewhat predisposed to urinary calculi formation, yet an additional genetic alteration, ie, elimination of Cav1, appears to promote accumulation of calcium microprecipitates in the calculi and ultimately frank urinary stones.

A causal factor as determined in our study was hypercalciuria in *Cav1*−/− males compared to *Cav1*+/+ males. There were no differences in urine calcium levels in the female mice further supporting hypercalciuria as the physiological determinant. Our immunohistochemistry studies indicated that Cav1 was predominately localized to the basolateral side of the DCT cells in wild-type mice and in *Cav1*−/− male and female mice the absence of Cav1 led to an aberrant distribution of PMCA (Figure 4) but did not affect the Na^+/Ca^{++} exchanger. Caveolae are important determinants of calcium transport and calcium-mediated signaling[2] and co-localization of Cav1 and calcium pumps have been reported in cells that morphologically lack caveolae.[34] As further confirmation of this molecular mechanism, our *in vivo* analysis, a Ca^{++}, Mg^{++}-deficient diet confirmed that *Cav1*−/− mice had a significant defect in active reabsorption of Ca^{++}. The specific association of urolithiasis with male but not female *Cav1*−/− mice is consistent with the limited information available for human stone disease but the underlying mechanisms were not completely resolved in this study. It is conceivable that this sex-associated phenomenon is related to the quantity (male mice of both geno-

types have two-fold more urinary total protein than female mice, see Table 1), or types of proteins present in male urine.[35] Alternatively, since urine Ca^{++} levels in *Cav1−/−* female mice did not differ from *Cav1+/+* mice, other hormone-regulated processes related to Ca^{++} transport may be involved. It seems unlikely that disruption of *Cav1* had effects on parathyroid hormone or vitamin D_3 signaling since serum Ca^{++} levels and the intracellular level of calbindin D_{28k} were unaffected.

Overall, our studies support a multigenic contribution in frank calcium urinary stone formation. They are consistent with an initial predisposing protein component that serves as a nidus and matrix for further microscopic calcium deposition. By elimination of Cav1, the progression of this process toward urinary stone formation occurs much more rapidly beginning with microscopic deposition of Ca^{++} and ultimately leading to frank ostensible stones. It is not clear whether the nature of the protein milieu is altered in *Cav1−/−* mice, and this will be the target of future studies. However, it is clear from our studies that the absence of Cav1 leads to hypercalciuria that appears to be secondary to mislocalization and likely misfunction of PMCA, an important calcium pump protein in the mouse distal nephron. Therefore, overall our results have further enlightened the process of stone formation and have potential clinical utility. Indeed, this mouse model system may be appropriate and useful for further studies that elucidate the molecular mechanisms underlying urolithiasis in humans.

Acknowledgments

We thank G. Schuster for injection of ES cells and Drs. T.M. Wheeler and M.M. Ittmann for pathological assistance.

References

1. Parton RG: Caveolae and caveolins. Curr Opin Cell Biol 1996, 8:542–48
2. Shaul PW, Anderson RG: Role of plasmalemmal caveolae in signal transduction. Am J Physiol 1998, 275:L843–851
3. Yang G, Truong LD, Timme TL, Ren C, Wheeler TM, Park SH, Nasu Y, Bangma CH, Kattan MW, Scardino PT, Thompson TC: Elevated expression of caveolin is associated with prostate and breast cancer. Clin Cancer Res 1998, 4:1873–1880
4. Nasu Y, Timme TL, Yang G, Bangma CH, Li L, Ren C, Park SH, DeLeon M, Wang J, Thompson TC: Suppression of caveolin expression induces androgen sensitivity in metastatic androgen-insensitive mouse prostate cancer cells. Nat Med 1998, 4:1062–1064
5. Yang G, Truong LD, Wheeler TM, Thompson TC: Caveolin-1 expression in clinically confined human prostate cancer: a novel prognostic marker. Cancer Res 1999, 59:5719–5723
6. Yang G, Addai J, Ittmann M, Wheeler TM, Thompson TC: Elevated caveolin-1 levels in African-American versus white-American prostate cancer. Clin Cancer Res 2000, 6:3430–3433
7. Tahir SA, Yang G, Ebara S, Timme TL, Satoh T, Li L, Goltsov A, Ittmann M, Morrisett JD, Thompson TC: Secreted caveolin-1 stimulates cell survival/clonal growth and contributes to metastasis in androgen-insensitive prostate cancer. Cancer Res 2001, 61:3882–3885
8. Scheinman SJ: Nephrolithiasis. Semin Nephrol 1999, 19:381–388
9. Borghi L, Schianchi T, Meschi T, Guerra A, Allegri F, Maggiore U, Novarini A: Comparison of two diets for the prevention of recurrent stones in idiopathic hypercalciuria. N Engl J Med 2002, 346:77–84
10. Piwon N, Gunther W, Schwake M, Bosl MR, Jentsch TJ: ClC-5 Cl-channel disruption impairs endocytosis in a mouse model for Dent's disease. Nature 2000, 408:369–373
11. Wang SS, Devuyst O, Courtoy PJ, Wang XT, Wang H, Wang Y, Thakker RV, Guggino S, Guggino WB: Mice lacking renal chloride channel, CLC-5, are a model for Dent's disease, a nephrolithiasis disorder associated with defective receptor-mediated endocytosis. Hum Mol Genet 2000, 9:2937–2945
12. Ramirez-Solis R, Davis AC, Bradley A: Gene targeting in embryonic stem cells. Methods Enzymol 1993, 225:855–878
13. Loffing J, Loffing-Cueni D, Valderrabano V, Klausli L, Hebert SC, Rossier BC, Hoenderop JG, Bindels RJ, Kaissling B: Distribution of transcellular calcium and sodium transport pathways along mouse distal nephron. Am J Physiol 2001, 281:F1021–F1027
14. Bancroft JD: Manual of Histological Techniques and Their Diagnostic Application. New York, Churchill Livingstone, 1994, pp 407–411
15. Wittner M, Jounier S, Deschenes G, de Rouffignac C, Di Stefano A: Cellular adaptation of the mouse cortical thick ascending limb of Henle's loop (CTAL) to dietary magnesium restriction: enhanced transepithelial Mg2+ and Ca2+ transport. Pflugers Arch 2000, 439: 765–771
16. Kogo H, Fujimoto T: Caveolin-1 isoforms are encoded by distinct mRNAs: identification of mouse caveolin-1 mRNA variants caused by alternative transcription initiation and splicing. FEBS Lett 2000, 465: 119–123
17. Drab M, Verkade P, Elger M, Kasper M, Lohn M, Lauterbach B, Menne J, Lindschau C, Mende F, Luft FC, Schedl A, Haller H, Kurzchalia TV: Loss of caveolae, vascular dysfunction, and pulmonary defects in caveolin-1 gene-disrupted mice. Science 2001, 293:2449–2452
18. Razani B, Combs TP, Wang XB, Frank PG, Park DS, Russell RG, Li M, Tang B, Jelicks LA, Scherer PE, Lisanti MP: Caveolin-1-deficient mice are lean, resistant to diet-induced obesity, and show hypertriglyceridemia with adipocyte abnormalities. J Biol Chem 2002, 277:8635–8647
19. Zhao YY, Liu Y, Stan RV, Fan L, Gu Y, Dalton N, Chu PH, Peterson K, Ross Jr J, Chien KR: Defects in caveolin-1 cause dilated cardiomyopathy and pulmonary hypertension in knockout mice. Proc Natl Acad Sci USA 2002, 99:11375–11380
20. Randall A: The etiology of primary renal calculus. Int Abstr Surg 1940, 71:209–240
21. Tamai O, Oka N, Kikuchi T, Koda Y, Soejima M, Wada Y, Fujisawa M, Tamaki K, Kawachi H, Shimizu F, Kimura H, Imaizumi T, Okuda S: Caveolae in mesangial cells and caveolin expression in mesangial proliferative glomerulonephritis. Kidney Int 2001, 59: 471–480
22. Breton S, Lisanti MP, Tyszkowski R, McLaughlin M, Brown D: Basolateral distribution of caveolin-1 in the kidney: absence from H+-atpase-coated endocytic vesicles in intercalated cells. J Histochem Cytochem 1998, 46:205–214
23. Hoenderop JG, Nilius B, Bindels RJ: Molecular mechanism of active Ca2+ reabsorption in the distal nephron. Annu Rev Physiol 2002, 64:529–549
24. Boyce WH: Organic matrix of human urinary concretions. Am J Med 1968, 45:673–683
25. Morse RM, Resnick MI: Urinary stone matrix. J Urol 1988, 139:602–606
26. Cerini C, Geider S, Dussol B, Hennequin C, Daudon M, Veesler S, Nitsche S, Boistelle R, Berthezene P, Dupuy P, Vazi A, Berland Y, Dagorn JC, Verdier JM: Nucleation of calcium oxalate crystals by albumin: involvement in the prevention of stone formation. Kidney Int 1999, 55:1776–1786
27. Tessier J, Petrucci M, Trouve ML, Valiquette L, Guay G, Ouimet D, Bonnardeaux A: A family-based study of metabolic phenotypes in calcium urolithiasis. Kidney Int 2001, 60:1141–1147
28. Curhan GC, Willett WC, Speizer FE, Stampfer MJ: Twenty-four-hour urine chemistries and the risk of kidney stones among women and men. Kidney Int 2001, 59:2290–2298
29. Levy FL, Adams-Huet B, Pak CY: Ambulatory evaluation of

nephrolithiasis: an update of a 1980 protocol. Am J Med 1995, 98:50–59
30. Bushinsky DA, Grynpas MD, Asplin JR: Effect of acidosis on urine supersaturation and stone formation in genetic hypercalciuric stone-forming rats. Kidney Int 2001, 59:1415–1423
31. Hoenderop JG, Willems PH, Bindels RJ: Toward a comprehensive molecular model of active calcium reabsorption. Am J Physiol Renal Physiol 2000, 278:F352–F360
32. Menon M, Resnick MI: Urinary lithiasis: etiology, diagnosis and medical management. Campbell's Urology. Edited by Walsh P, Retik A, Vaughan D, Wein A. New York, Elsevier Science, 2003, 4:3227–3305
33. McGaughey C: Excretion of uncrystallized urinary calculi composed of glyco-protein by normal and muscular dystrophic mice. Nature 1961, 192:1267–1269
34. Fujimoto T: Calcium pump of the plasma membrane is localized in caveolae. J Cell Biol 1993, 120:1147–1157
35. Hastie ND, Held WA, Toole JJ: Multiple genes coding for the androgen-regulated major urinary proteins of the mouse. Cell 1979, 17: 449–457